Characterization of a Murine Cytomegalovirus Class I Major Histocompatibility Complex (MHC) Homolog: Comparison to MHC Molecules and to the Human Cytomegalovirus MHC Homolog

TARA L. CHAPMAN[1] AND PAMELA J. BJORKMAN[1,2]*

*Division of Biology 156-29[1] and Howard Hughes Medical Institute,[2]
California Institute of Technology, Pasadena, California 91125*

Both human and murine cytomegaloviruses (HCMV and MCMV) down-regulate expression of conventional class I major histocompatibility complex (MHC) molecules at the surfaces of infected cells. This allows the infected cells to evade recognition by cytotoxic T cells but leaves them susceptible to natural killer cells, which lyse cells that lack class I molecules. Both HCMV and MCMV encode class I MHC heavy-chain homologs that may function in immune response evasion. We previously showed that a soluble form of the HCMV class I homolog (U_L18) expressed in Chinese hamster ovary cells binds the class I MHC light-chain β2-microglobulin and a mixture of endogenous peptides (M. L. Fahnestock, J. L. Johnson, R. M. R. Feldman, J. M. Neveu, W. S. Lane, and P. J. Bjorkman, Immunity 3:583–590, 1995). Consistent with this observation, sequence comparisons suggest that U_L18 contains the well-characterized groove that serves as the binding site in MHC molecules for peptides derived from endogenous and foreign proteins. By contrast, the MCMV homolog (m144) contains a substantial deletion within the counterpart of its α2 domain and might not be expected to contain a groove capable of binding peptides. We have now expressed a soluble version of m144 and verified that it forms a heavy chain–β2-microglobulin complex. By contrast to U_L18 and classical class I MHC molecules, m144 does not associate with endogenous peptides yet is thermally stable. These results suggest that U_L18 and m144 differ structurally and might therefore serve different functions for their respective viruses.

Cytomegaloviruses (CMVs) are ubiquitous, host-specific pathogens that are capable of establishing lifelong infections in immunocompetent hosts. Although acute infection will elicit an immune response, this response usually fails to completely resolve the infection. Instead, the virus persists in the host, often in a state of latency, and recurrent infections may be observed if the animal becomes immunocompromised (5). In order to maintain this degree of persistence, especially in the face of a fully primed immune system, CMVs have developed various means of modulating the host immune system. One strategy used by both human and murine CMVs (HCMV and MCMV) is the down-regulation of host class I major histocompatibility complex (MHC) molecules (6). Class I MHC molecules are polymorphic glycoproteins composed of a membrane-bound heavy chain associated with a nonpolymorphic light chain, β2-microglobulin (β2m). Class I molecules present peptides derived from the degradation of cytoplasmic proteins to cytotoxic T cells, thus enabling them to survey the status of the interior of the cell (49). In an uninfected cell, MHC molecules bind peptides derived from self proteins to which T cells are tolerant. However, in an infected cell, some MHC molecules are occupied by peptides derived from viral proteins, to which T cells react by killing the cell. By down-regulating MHC class I molecules, viruses are able to elude viral-antigen-specific cytotoxic T cells.

Although interference with class I-mediated antigen presentation or class I expression may enable infected cells to evade virus-specific T cells, it may also render these cells susceptible to detection and lysis by NK cells. NK cells express both activating and inhibitory surface receptors (31). The activating receptors are predominantly triggered by non-MHC molecules, while the inhibitory receptors recognize class I MHC molecules (31). Stimulation of activating receptors leads to target cell lysis unless the NK cell inhibitory receptors are able to engage an adequate level of self class I molecules on the target cell (27). Therefore, those cells that have down-regulated their class I molecules to a level sufficient to avoid T cells can be recognized and eliminated by NK cells.

As a possible means of undermining the host NK cell response, both HCMV and MCMV encode MHC class I homologs (2, 14, 39). It has been hypothesized that the role of these homologs in a virus-infected cell is to engage NK cell inhibitory receptors, thereby preventing the lysis that would normally occur due to down-regulation of class I molecules (11, 14, 40). In this way virus-infected cells are less susceptible to lysis by both cytotoxic T lymphocytes and NK cells. The HCMV-encoded homolog, U_L18, is a 348-residue type I transmembrane glycoprotein whose extracellular region shares ~25% amino acid sequence identity with the extracellular regions of human class I molecules (2) (Fig. 1A). Like class I MHC molecules, U_L18 associates with β2m (6). We previously showed that a soluble form of U_L18 expressed in Chinese hamster ovary (CHO) cells binds a mixture of endogenous peptides with characteristics similar to those of peptides eluted from class I molecules, that is, "anchor" residues, and a predominance of short peptides derived from cytoplasmic proteins (11). The MCMV-encoded MHC homolog, m144, is a 383-residue type I transmembrane glycoprotein whose extracellular region shares ~25% amino acid sequence identity with the corresponding part of murine class I MHC extracellular re-
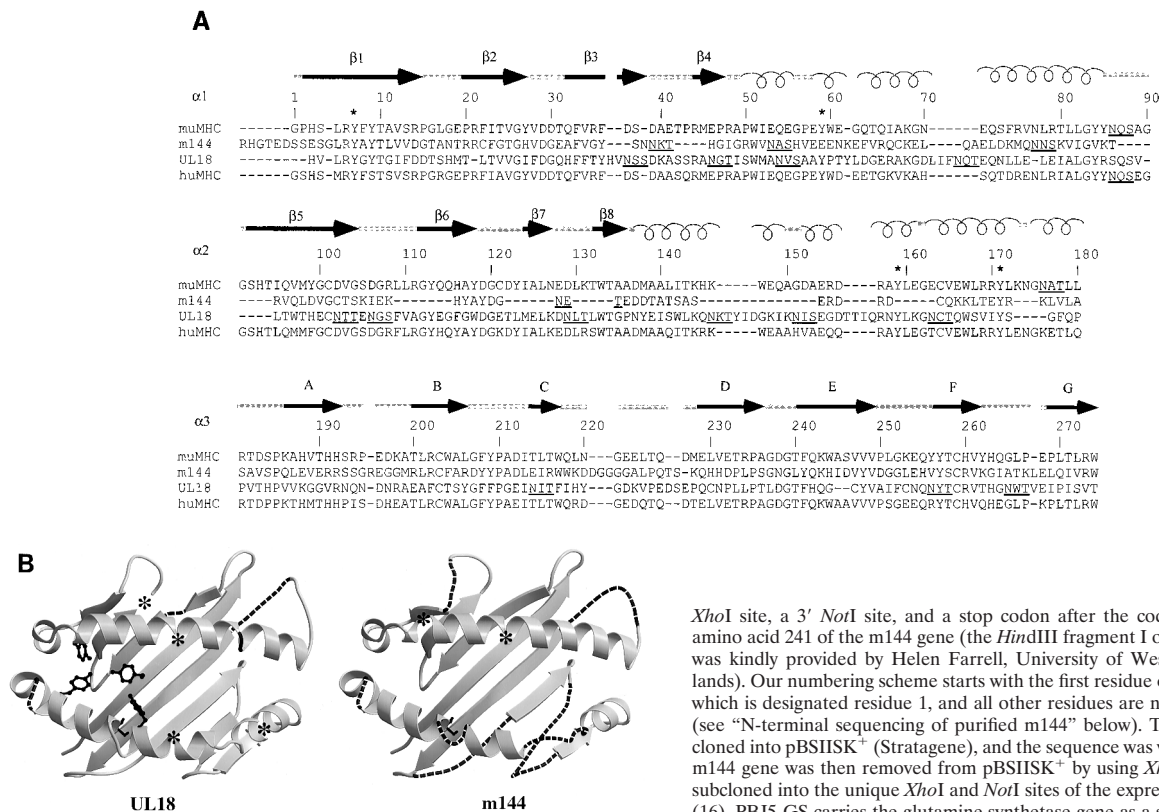
A

B

UL18   m144

FIG. 1. Comparison of MCMV and HCMV class I homologs with class I MHC molecules. (A) Sequence alignment of the mature extracellular regions of m144 with a murine class I molecule (muMHC) and of U$_L$18 with a human class I MHC molecule (huMHC) (based on data from Fig. 1 in reference 14). Numbering is with reference to class I MHC molecules. Crystallographically determined secondary-structural elements in class I MHC molecules (3) are shown above the sequences as arrows for β strands (strands 1 through 8 within the α1 and α2 domains are labeled β1 to β8, and strands 1 through 7 within the α3 domain are labeled A to G) and spirals for α-helical regions. Positions of conserved tyrosines in the pocket that accommodates peptide N termini (pocket A in class I MHC molecules [45, 47]) are marked with an asterisk, and potential N-linked glycosylation sites are underlined. (B) Locations of U$_L$18 and m144 sequence insertions and deletions on the class I MHC structure. Ribbon diagrams of the carbon-α backbone of the α1 and α2 domains of HLA-A2 (4, 45) are shown with the locations of U$_L$18 or m144 insertions indicated by asterisks; class I regions that are deleted in U$_L$18 or m144 are indicated by dashed lines. Conserved tyrosines shared between U$_L$18 and class I molecules are highlighted in the left panel. This figure was generated by using Molscript (28) and Raster-3D (34).

gions (14, 39) (Fig. 1A). The two viral homologs are not closely related to each other, sharing only 18% sequence identity, thus requiring that m144 be separately characterized.

In this paper we describe the expression and biochemical characterization of a soluble version of m144. We find that, like U$_L$18 and class I MHC molecules, m144 binds β2m, but unlike these other proteins, it does not associate with endogenous peptides. We further demonstrate that m144 is thermally stable in the absence of bound peptide, unlike both class I MHC molecules (13, 33, 46, 50) and U$_L$18. Taken together with a sequence comparison of m144 with class I MHC molecules, these results suggest that the m144 counterpart of the MHC peptide-binding site differs from those of both class I molecules and U$_L$18 (Fig. 1B).

MATERIALS AND METHODS

Construction of the m144 expression plasmid. Molecular cloning manipulations were performed by standard protocols (43). PCR was used to insert a 5′

Xho I site, a 3′ Not I site, and a stop codon after the codon corresponding to amino acid 241 of the m144 gene (the Hind III fragment I of MCMV strain K181 was kindly provided by Helen Farrell, University of Western Australia, Nedlands). Our numbering scheme starts with the first residue of the mature protein, which is designated residue 1, and all other residues are numbered sequentially (see "N-terminal sequencing of purified m144" below). The PCR product was cloned into pBSIISK$^+$ (Stratagene), and the sequence was verified. The modified m144 gene was then removed from pBSIISK$^+$ by using Xho I and Not I and was subcloned into the unique Xho I and Not I sites of the expression vector PBJ5-GS (16). PBJ5-GS carries the glutamine synthetase gene as a selectable marker and as a means of gene amplification in the presence of the drug methionine sulfoximine, a system developed by Celltech (1).

Construction of the murine β2m (b allele) expression plasmid. An expression plasmid containing the a allele of murine β2m (mβ2m^a) was previously constructed in our laboratory (12). This allele of β2m, however, is not recognized by the anti-mβ2m monoclonal antibody (MAb) S19.8 (48). Originally anticipating that m144-mβ2m heterodimers could be purified by S19.8 immunoaffinity chromatography, we used site-directed mutagenesis to change mβ2m^a to mβ2m^b. This mβ2m^a gene was excised by using Xba I and Xho I and was subcloned into the same sites in pBSKS+ (Stratagene). The a and b alleles of mβ2m differ by only 1 nucleotide, which changes residue 85 from Asp to Ala (15). The single nucleotide was altered by oligonucleotide-directed in vitro mutagenesis (29), and the sequence was verified. The modified mβ2m gene was then removed from pB-SKS$^+$ by using Xba I and Xho I and was subcloned into the unique Xba I and Xho I sites of the expression vector PBJ1 (32). Unfortunately, the mβ2m^b epitope recognized by the antibody S19.8 is inaccessible when the protein is complexed to the m144 heavy chain, as verified in immunoprecipitation experiments (data not shown).

Cell culture and transfection. The m144 expression plasmid was cotransfected with either a human β2m (hβ2m) (13) expression vector or the previously described mβ2m expression vector into CHO cells by a Lipofectin procedure (GIBCO BRL). Cells resistant to 100 μM methionine sulfoximine were selected according to the protocol established by Celltech, modification of which has been previously described (16). Transfected CHO cells were maintained in glutamine-free α minimal essential medium (Irvine Scientific) supplemented with 5% dialyzed fetal bovine serum (GIBCO BRL), 100 μM methionine sulfoximine (Sigma), penicillin (100 U/ml), and streptomycin (100 μg/ml). Cells secreting m144-β2m heterodimers were identified by immunoprecipitation of supernatants of cells metabolically labeled with [^{35}S]methionine and [^{35}S]cysteine (see below) by using either an antibody against hβ2m (BBM.1) (36) or anti-m144 antiserum. Clones were considered positive if immunoprecipitation yielded a heavy chain of 44 kDa and a light chain of 12 kDa. The heavy chain was verified to be m144 by N-terminal sequencing (see below).

^{35}S metabolic labeling. m144-transfected CHO cell lines derived from colonies were expanded into 12-well trays, grown to confluence, and incubated for 5 h in 1.0 ml of methionine- and cysteine-free medium (GIBCO BRL) plus 1% dialyzed fetal bovine serum including 5 μCi of a [^{35}S]methionine and [^{35}S]cysteine (ICN) mixture. Supernatants were clarified by a 5-min spin in a microcentrifuge, and either BBM.1 or anti-m144 antiserum (see below) was added. Immunoprecipitations were carried out by standard methods (21) with protein G-bearing Sepharose beads (Pharmacia). Samples were boiled in sodium dodecyl sulfate-polyacrylamide gel electrophoresis (SDS-PAGE) running buffer and loaded onto 15% polyacrylamide gels, which were fixed, dried, and exposed to a Phosphor-

Imager screen (Molecular Dynamics). The image was then developed with a Molecular Dynamics 425E phosphorimage scanner.

Protein purification. m144-hβ2m- and m144-mβ2m-secreting CHO cell lines were grown to confluence in 50 10-cm plates. Supernatants were collected every 3 days for 1 month. Soluble m144-hβ2m heterodimers were purified from the supernatants on a BBM.1 immunoaffinity column. This affinity column was prepared by coupling 70 mg of the BBM.1 MAb to cyanogen bromide-treated Sepharose 4B (Pharmacia) at approximately 10 mg of antibody/ml of resin according to the protocol of the manufacturer. Supernatants were passed over the affinity column, which was then washed with 50 column volumes of a solution consisting of 50 mM Tris (pH 7.4), 0.1% NaN₃, and 1 mM EDTA. Free β2m and m144-hβ2m heterodimers were eluted from the BBM.1 column with 50 mM diethylamine (pH 11.5) into tubes containing 1.0 M Tris (pH 7.4). Free hβ2m was separated from m144-hβ2m heterodimers by using a Superdex 200 HR 10/30 fast protein liquid chromatography (FPLC) filtration column. Approximately 3 mg of m144-hβ2m heterodimers was recovered per liter of transfected cell supernatants. Soluble m144-mβ2m heterodimers were purified from the supernatants on a 15C6 immunoaffinity column made by coupling an anti-m144 MAb (see below) to Sepharose beads as described above. Supernatants from m144-mβ2m-secreting CHO cell lines were passed over the column, the column was washed, and the protein was eluted as described above. A second protein migrating with an apparent molecular mass of 93 kDa coeluted with the m144-mβ2m heterodimer and was separated by using a Superdex 200 HR 10/30 FPLC filtration column. Approximately 1 mg of m144-mβ2m heterodimer was recovered per liter of transfected cell supernatants.

N-terminal sequencing of purified m144. N-terminal sequencing was performed on 2.3 µg of purified soluble m144-hβ2m or m144-mβ2m in a phosphate buffer dried onto a poly(vinylidene difluoride) membrane and inserted into an Applied Biosystems model 476A sequencer reaction cartridge. Two sequences were isolated from the m144-hβ2m sample: the sequence IQRTPKIQVYSRH PAEN, corresponding to the first 17 residues of mature hβ2m (26), and the sequence HGTEDSSESGLRYAYT, corresponding to the first 17 residues of the mature m144 heavy chain (reference 14 and data not shown). Two sequences were also isolated from the m144-mβ2m sample: the sequence IQKTPQIQVYS RHPPEN, corresponding to the first 17 residues of mature mβ2m (17), and the residues given above for the m144 heavy chain.

Acid elution and characterization of peptides. Purified secreted U_L18, m144-hβ2m, m144-mβ2m, FcRn (a class I MHC homolog that functions as a receptor for the Fc portions of immunoglobulin G [16]), and H2-K^d-hβ2m (a murine class I MHC heavy chain complexed with hβ2m [13]) proteins were analyzed for the presence of bound peptides. All these proteins were produced in CHO cells as described above for m144. In these experiments, FcRn served as the negative control, since it had previously been established by biochemical and crystallographic methods that it does not associate with endogenous peptides (7, 37), while U_L18 and K^d served as positive controls, since endogenous peptides had previously been characterized from samples of these proteins (11, 37). Acid elutions and sequencing were performed by established methods (24, 42, 51). Briefly, 0.25 mg of protein was concentrated to 100 µl in a Centricon 3 (molecular weight cutoff, 3,000) ultrafiltration device (Amicon; Beverly, Mass.). After dilution with 1.0 ml of 50 mM ammonium acetate (pH 7.5), the proteins were again concentrated to 100 µl, and this procedure was repeated. The washed protein was then treated with 1.0 ml of 12% acetic acid, heated to 70°C for 5 min, and subsequently concentrated again to 100 µl in the ultrafiltration unit, with the filtrate containing any eluted material. This elution step was then repeated. The acid eluates were lyophilized and analyzed by automated Edman degradation with an Applied Biosystems model 476A protein sequencer (see Table 1). Eluates were also analyzed with a Perkin-Elmer/Applied Biosystems Inc. model 172A microbore high-pressure liquid chromatograph (HPLC) and a Reliasil C₁₈ (Reliasil Column Engineering) column. Material was eluted by using a 3-ml gradient from 0.05% trifluoroacetic acid in water to 0.05% trifluoroacetic acid in 40% acetonitrile. Absorbance was monitored at 200 nm. The fractions containing peaks were analyzed by matrix-assisted, laser desorption, time-of-flight mass spectrometry with a PerSeptive Biosystems (Farmingham, Mass.) ELITE mass spectrometer.

CD analyses. An Aviv 62A DS spectropolarimeter equipped with a thermoelectric cell holder was used for circular dichroism (CD) measurements. Wavelength scans and thermal denaturation curves were obtained from samples containing 10 µM protein in 5 mM phosphate at pH 7 by using a 0.1-mm path length cell for wavelength scans and a 1-mm path length cell for thermal denaturation measurements. The heat-induced unfolding of U_L18, m144-hβ2m, m144-mβ2m, and H2-K^d-hβ2m was monitored by recording the CD signal at 223 nm while the sample temperature was raised from 25 to 75°C at a rate of approximately 0.7°C/min. The transition midpoint (T_m) for each curve was determined by taking the maximum of a plot of $d\theta/dT$ versus T (where θ is ellipticity) after averaging the data with a moving window of 5 points.

Production of MAbs and polyclonal antiserum. Three MAbs were generated for the studies presented here, two specific for m144-β2m and one specific for the U_L18 heavy chain. Of those that recognize m144-β2m, 15C6 was raised against a gel slice of the m144 heavy chain and 19G4 was raised against the m144-hβ2m heterodimer. Female BALB/c mice (5 weeks old) were primed and twice boosted at 2-week intervals by intraperitoneal injection of either a 5- by 10- by 1.5-mm homogenized gel slice containing m144 or 100 µg of purified soluble m144-hβ2m. Serum was screened 1 week after each injection by enzyme-linked immu-

nosorbent assay (ELISA). Three days preceding the fusion, one mouse was boosted with a gel slice or 100 µg of purified m144 in phosphate-buffered saline. Splenocytes from the boosted mouse were fused with HL-1 murine myeloma cells, and media from the hybridoma cultures were tested for antibodies against the m144 heavy chain by ELISA. After subcloning of positive clones at clonal density, ascites tumors were produced in pristane-primed BALB/c mice. In addition, a rabbit antiserum recognizing m144 was raised against a gel slice of the m144 heavy chain (Antibodies Incorporated, Davis, Calif.). Both MAbs and the antiserum are effective reagents in an ELISA for detection of m144-β2m, immunoprecipitation of soluble m144-β2m heterodimers, and Western blotting. The U_L18-specific MAb, 10C7, was prepared similarly to m144-specific MAbs; however, the mice used were female OLA × BL6 hβ2m transgenic mice (a kind gift of H. Ploegh, Massachusetts Institute of Technology) injected with enzymatically deglycosylated U_L18-β2m heterodimers. Several previous attempts to isolate an antibody against the U_L18 heavy chain in nontransgenic mice failed, presumably because U_L18 is heavily glycosylated (13 potential N-linked glycosylation sites [2]), so that an antibody recognizing a protein epitope within U_L18 rather than β2m was difficult to isolate. Indeed, all hybridomas screened from nontransgenic mice produced antibodies that recognized hβ2m instead of the heavy chain. By using hβ2m transgenic mice, many potential MAbs against the heavy chain were generated. A rabbit antiserum recognizing U_L18 was raised against a gel slice of the U_L18 heavy chain (HRP Inc., Denver, Pa.). Both the MAb and the antiserum are effective reagents in an ELISA for detection of U_L18-hβ2m, immunoprecipitation of soluble U_L18-hβ2m heterodimers, and Western blotting.

Preparation of peptide-filled U_L18 and H-2K^d. U_L18 was purified from the supernatants of U_L18-hβ2m-secreting cells (11) grown in a hollow-fiber bioreactor device (Cell Pharm I; Unisyn Fibertec, San Diego, Calif.). Using this system, only 35 to 40% of the molecules appear to contain endogenous peptides, compared to U_L18 produced from transfected cells grown on plates, which appears to be fully occupied (11). As previously described (11), we calculated the percent of U_L18 occupied with peptide by comparing the amount of peptide material eluted from K^d with the amount eluted from U_L18 when the number of picomoles of starting protein is the same. The peptide ALPHAILRL, previously identified as a major component of U_L18 acid eluates (11), was synthesized with an Applied Biosystems 433A peptide synthesizer. The peptide was incubated with U_L18 at a 20:1 molar ratio for 12 h at room temperature. Unbound peptides were separated from U_L18 by passing the mixture over a Superdex 200 HR 10/30 FPLC size exclusion column. H-2K^d was purified from supernatants of K^d-hβ2m-secreting cells grown on 10-cm plates. Previous characterization of soluble K^d established that ∼70% of the protein is empty and ∼30% is occupied by endogenous peptide (13). The peptide SYIPSAEKI, previously identified as a K^d-binding peptide (12, 41), was synthesized and incubated with partially empty K^d, and unbound peptide was separated from K^d-peptide complexes as described above for preparation of peptide-filled U_L18.

RESULTS

Soluble m144 associates with hβ2m and mβ2m. To investigate whether m144 binds β2m and serves as a peptide receptor, we expressed a soluble version of m144 in CHO cells together with hβ2m or mβ2m. The soluble version of m144 was constructed by truncating the gene prior to the predicted transmembrane region (following residue 241 of the mature protein). Initial experiments were performed with the hβ2m gene in order to facilitate detection of the protein product with the antibody BBM.1 (36), which binds to hβ2m but not to mβ2m. Transfected cells were screened by immunoprecipitating metabolically labeled supernatants with BBM.1. SDS-PAGE analysis of protein from positive clones revealed two bands, one having an apparent molecular mass of 45 kDa (consistent with its identity as truncated m144) and the other having an apparent molecular mass of 12 kDa, corresponding to β2m. The calculated molecular mass of truncated m144 is 27 kDa, but the protein is glycosylated (4 potential N-linked glycosylation sites [14, 39]) and would be expected to migrate with a higher apparent molecular mass. Supernatants from positive clones were passed over a BBM.1 immunoaffinity column, eluted, then passed over a size exclusion column to separate free β2m from β2m-heavy chain heterodimers. An SDS-PAGE gel of the resulting purified protein is shown in Fig. 2. N-terminal sequencing of purified heterodimers confirmed the sequences of the first 17 residues of the mature forms of hβ2m (26) and m144 (14, 39).
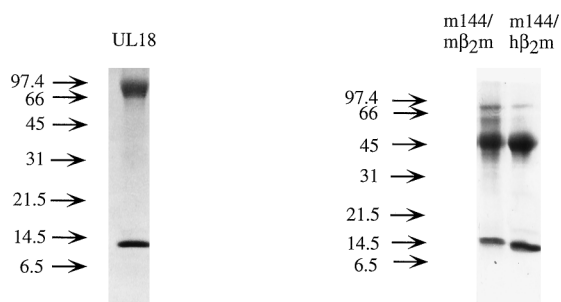
Soluble m144 was used to produce MAbs that could be used

FIG. 2. SDS-PAGE (15% polyacrylamide) analysis of U_L18 and the two forms of m144. Proteins were purified from the supernatants of transfected CHO cells by passage over an immunoaffinity column followed by size exclusion chromatography. The heavy chains of both heterodimers migrate with a higher apparent molecular mass than is suggested by the mass of their protein backbones due to the addition of N-linked glycosides (U_L18 contains 13, and m144 contains 4, potential N-linked glycosylation sites).

to recognize m144 when complexed with mβ2m. Two antibodies were produced: 15C6, which was raised against a gel slice of the m144 heavy chain, and 19G4, which was raised against purified m144-hβ2m heterodimers. CHO cells were transfected with genes encoding truncated m144 and the b allele of mβ2m. Cells expressing m144-mβ2m heterodimers could be identified by immunoprecipitation with either the anti-m144 MAbs or a polyclonal anti-β2m antiserum that recognizes mβ2m, but not by immunoprecipitation with the MAb S19.8 (48), which apparently does not react with mβ2m^b complexed with m144. SDS-PAGE analysis of immunoprecipitated protein from cells expressing m144 and mβ2m also reveals two bands migrating at 45 and 12 kDa (data not shown). m144-mβ2m was purified from transfected cell supernatants on an immunoaffinity column constructed with MAb 15C6 (Fig. 2). N-terminal sequencing of purified protein established that the heterodimer was composed of the mature forms of m144 and mβ2m. Sequences of hamster (16) and bovine (20) β2m were not detected, indicating that m144 was not associating with endogenous hamster β2m or exchanging with bovine β2m in the medium, as can occur when mouse class I MHC proteins are expressed with mβ2m in CHO cells (13).

m144 does not bind endogenous peptides. To determine if either m144-hβ2m or m144-mβ2m binds peptides, purified proteins were treated with acetic acid to dissociate potential peptide material (24, 42, 51). Acid eluates were characterized by N-terminal sequencing (see Table 1), HPLC, and mass spectrometry. Soluble versions of other proteins expressed in CHO cells (the murine class I MHC molecule H2-K^d and two other MHC class I homologs, U_L18 from HCMV and the rat neonatal Fc receptor, FcRn) were subjected to the same treatment. K^d and U_L18 had previously been shown to bind peptides and were used as positive controls (10, 11, 37). FcRn does not bind peptides (7, 37) and was used as a negative control.

The characteristics of the peptides isolated from K^d and U_L18 were similar to those previously reported (11, 37) and consistent with the known requirement for a tyrosine anchor at position 2 for K^d (38) and a leucine or methionine anchor at position 2 for U_L18 (11) (Table 1). An aliquot of the U_L18 acid eluate was passed over a reverse-phase HPLC column, several peaks were collected, and a number of these were characterized by mass spectrometry. This procedure resulted in identification of multiple peptides in the U_L18 acid eluate whose exact molecular weights corresponded to the sequences of peptides previously shown to be associated with U_L18 (reference 11 and data not shown).

By contrast, the low-molecular-weight acid eluates from m144-hβ2m, m144-mβ2m, and FcRn did not show the presence of peptides (Table 1). With the exception of cycle 1, which is typically subject to high backgrounds, the total yield of the amino acids from each cycle of pool sequencing of the acid eluates remained nearly constant, and this yield was only slightly above background. In addition, most of the peaks in the HPLC profile of the m144-hβ2m acid eluate were also apparent in eluates extracted from FcRn, and all were barely notable above the background. When the few peaks that differed between the m144-hβm and FcRn eluates were collected and characterized by mass spectrometry, these peaks were found to contain low-molecular-weight material that did not show proteinaceous characteristics (data not shown).

m144, but not U_L18, is thermally stable in the absence of peptides. Class I MHC heavy chains show decreased stability in the absence of bound peptide (13, 33, 50). To ascertain if m144-hβ2m or m144-mβ2m is unstable due to the absence of bound peptide, we monitored the heat-induced unfolding of these proteins by recording the CD signal at 223 nm while increasing the sample temperature from 25 to 75°C (Fig. 3A). The results were compared with melting curves of partially empty and peptide-filled forms of the class I MHC molecule H-2K^d (Fig. 3B) (13). Two unfolding transitions are evident in the curve derived from m144-hβ2m. The first, with a T_m of 55°C, corresponds to the unfolding of the m144 heavy chain, while the second, with a T_m of 64°C, corresponds to the previously observed T_m for hβ2m (13) and represents the independent unfolding of the light chain subsequent to heavy-chain denaturation. m144-mβ2m melts less cooperatively than m144-hβ2m and the derived T_m for the heavy-chain unfolding (52°C) is slightly lower, indicating that m144 complexed with mβ2m is somewhat less stable than m144 complexed with hβ2m. In addition, the downward-sloping transition for the melting of β2m is not apparent in the melting curve of m144-mβ2m, perhaps being obscured by the CD signal from the melted m144 heavy chain. Similar results were obtained for the melting of K^d complexed with mβ2m (12). The melting behavior of

TABLE 1. Amino acids recovered from acid elutions^a

Cycle	Yield (pmol) of:				
	U_L18	H-2K^d-hβ2m	FcRn	m144-hβ2m	m144-mβ2m^b
1	86	84.5	5.9	13.7	7.3
2	75.1^c	51.1^d	4.7	0	1.5
3	36.9^e	33.6	0.7	0.5	0.3
4	19.8	12.3	7.6	1.2	0.3
5	11.3	18.2	0	0.7	0.2
6	4.0	30.8	0	1.0	0.1
7	3.7	1.1	0.2	1.6	0.1
8	6.5	3.1	0.6	2.0	1.6
9	4.3	12.1	9.5	0.2	0.3
10	1.3	7.5	0.3	0.1	1.2
11	0.4	10.1	0.5	0.3	0.2
12	2.5	6.7	0.8	0.1	0.5

^{a} The total yield of amino acids from each sequencing cycle is presented for acid eluates derived from equivalent amounts of soluble U_L18, K^d-hβ2m, FcRn, m144-hβ2m, and m144-mβ2m heterodimers. Only those amino acid residues that showed an increase in the absolute amount recovered compared to the previous cycle were considered significant. Results for the FcRn, K^d, and U_L18 eluates are similar to those previously reported (11, 37) in which soluble U_L18 and K^d, but not FcRn, were shown to bind endogenous peptides.
^{b} Acid elution contributions from Asp, Glu, and Gly were not included in the m144-mβ2m tabulation because the first four cycles showed unusually high yields that were also present in the negative control.
^{c} Leu, Met = 71.
^{d} Tyr = 25.
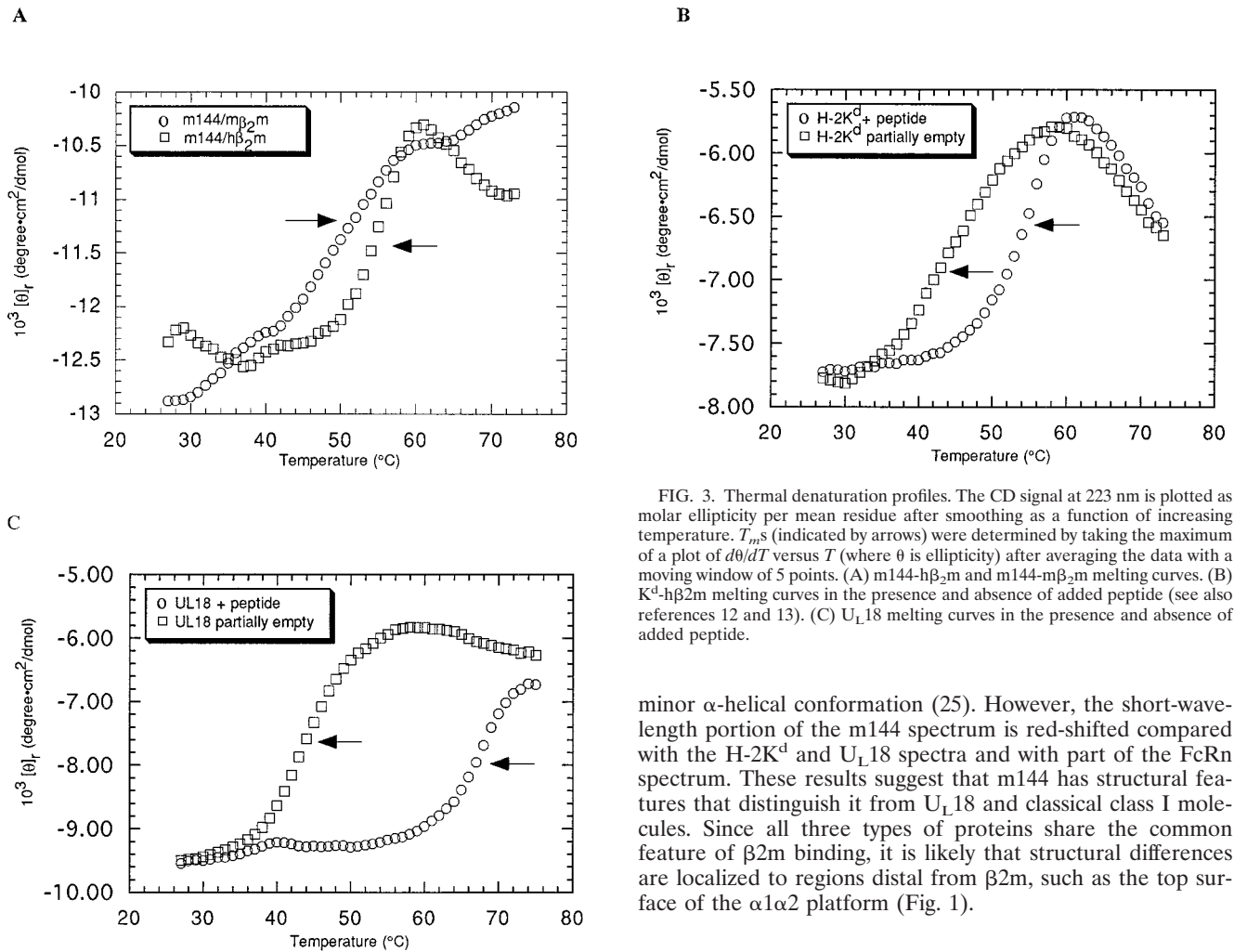^{e} Pro = 19.

A

B

FIG. 3. Thermal denaturation profiles. The CD signal at 223 nm is plotted as molar ellipticity per mean residue after smoothing as a function of increasing temperature. T_ms (indicated by arrows) were determined by taking the maximum of a plot of $d\theta/dT$ versus T (where θ is ellipticity) after averaging the data with a moving window of 5 points. (A) m144-hβ_2m and m144-mβ_2m melting curves. (B) K^d-hβ2m melting curves in the presence and absence of added peptide (see also references 12 and 13). (C) U$_L$18 melting curves in the presence and absence of added peptide.

C

minor α-helical conformation (25). However, the short-wavelength portion of the m144 spectrum is red-shifted compared with the H-2K^d and U$_L$18 spectra and with part of the FcRn spectrum. These results suggest that m144 has structural features that distinguish it from U$_L$18 and classical class I molecules. Since all three types of proteins share the common feature of β2m binding, it is likely that structural differences are localized to regions distal from β2m, such as the top surface of the α1α2 platform (Fig. 1).

DISCUSSION

HCMV and MCMV both encode class I MHC homologs. Previous studies indicated that U$_L$18, the HCMV class I homolog, binds the class I light chain β2m (6) and associates with endogenous peptides (11). In this study, we expressed a soluble version of the MCMV class I homolog m144 and compared its biochemical characteristics to those of class I molecules and U$_L$18. We found that m144 expressed in CHO cells associates with both hβ2m and mβ2m, implying that m144 heterodimerizes with host-derived β2m in virus-infected cells. However, unlike U$_L$18 and class I molecules, m144 does not bind endogenous peptides, since we do not detect peptide material associated with either form of m144-β2m. Other class I MHC homologs for which biochemical or structural studies do not reveal the presence of endogenous peptides include FcRn (7, 37), human Zn-α2-glycoprotein (44), and the hemochromatosis gene product HFE (31a). In addition, human MICA and mouse H-2T region-encoded molecules are stably expressed in cells that lack a functional peptide transporter, suggesting that they too do not bind conventional class I peptide ligands (9, 19, 23, 52).

A comparison of alignments of the m144 and U$_L$18 sequences with class I MHC sequences reveals that U$_L$18 is more likely than m144 to adopt a fold that includes an MHC-like peptide-binding groove (Fig. 1B). Peptides bind to class I MHC molecules in a groove located between two α-helices that span an 8-stranded β-pleated sheet. Peptide termini are
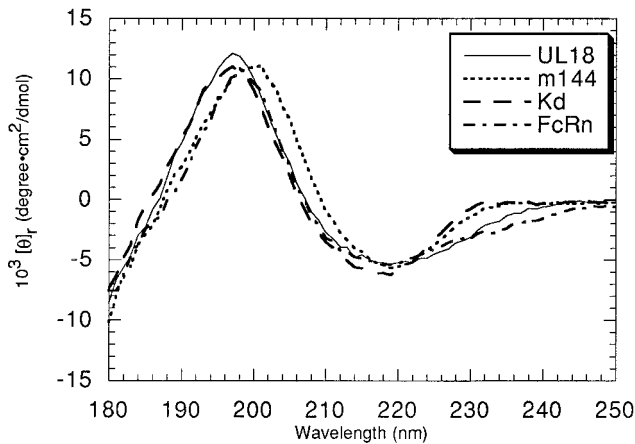
both forms of m144 is more similar to that of peptide-filled K^d ($T_m = 56°C$ for K^d-mβ2m; $T_m = 57°C$ for K^d-hβ2m) than to that of empty K^d ($T_m = 42°C$ for K^d-mβ2m; $T_m = 45°C$ for K^d-hβ2m) (12, 13) (compare Fig. 3A and B), suggesting that m144 is thermally stable in the absence of peptide.

By contrast, thermal-stability profiles of U$_L$18 indicate that U$_L$18 is only marginally stable in the absence of added peptide (Fig. 3C). The U$_L$18 protein produced from transfected CHO cells grown in a hollow-fiber bioreactor is estimated to be only 40% occupied with endogenous peptide (see Materials and Methods). This form of U$_L$18 melts with a T_m of 41°C. Upon addition of a known U$_L$18-binding peptide (11), the T_m increases to 66°C (Fig. 3C).

CD spectral comparison of m144, U$_L$18, FcRn, and class I MHC. The far-UV CD spectrum of m144 was compared with spectra of other MHC homologs and a classical class I molecule (Fig. 4). Far-UV CD spectra were previously used to characterize the secondary structures of class I MHC molecules and FcRn (16, 18, 30). The available crystal structures of FcRn and class I molecules (7, 47) can be used to verify the conclusion derived from the CD spectra that the secondary-structure arrangement of FcRn resembles, but is not identical to, class I MHC structures. The spectra of all four molecules (m144-hβ2m, U$_L$18, FcRn, and H-2K^d) show characteristics of proteins that are composed primarily of β-structure with a

FIG. 4. Far-UV CD spectra of peptide-filled U_L18, peptide-filled K^d, FcRn, and m144 expressed as ellipticity per mean residue. CD spectra of the partially empty versions of U_L18 and K^d superimpose almost perfectly upon spectra of their peptide-filled counterparts (data not shown).

accommodated in pockets at each end of the groove that are lined with conserved residues (reviewed in reference 47). The peptide N terminus binds in pocket A on the left side of the groove (as depicted in Fig. 1B), in which four conserved tyrosines make critical hydrogen bonds to main-chain atoms of the peptide (residues 7, 59, 159, and 171; class I numbering) (Fig. 1A). These tyrosines are also found in the U_L18 sequence, suggesting a similar mechanism for interaction with peptide N termini (11). While the U_L18 sequence shows some gaps and insertions compared to class I sequences, these are primarily confined to regions corresponding to the right side of the groove and suggest that the U_L18 structure may differ from MHC structures in the region of the groove that interacts with peptide C termini. Indeed, analysis of endogenous peptides associated with U_L18 revealed variability in the length of bound peptides (11), whereas classical class I molecules show a strong preference for binding octamer and nonamer peptides (reviewed in reference 47). By contrast, only two of the four pocket A tyrosines are conserved in the m144 sequence (Fig. 1A). Furthermore, the $\alpha2$ domain of m144 is significantly truncated compared to those of class I and U_L18 molecules, such that β strands 6 and 8 are much shorter, there is no predicted seventh strand, and there is a large deletion within the predicted $\alpha2$ domain helix. These characteristics do not seem compatible with formation of a functional peptide-binding groove, and they imply that this region of m144 is structurally distinct from class I molecules and U_L18. Far-UV CD spectral differences support this prediction (Fig. 4).

Our finding that m144, unlike class I MHC molecules and U_L18, is thermally stable in the absence of bound peptide is also consistent with a structural rearrangement in the counterpart of its peptide-binding region. CD melting curves of m144 complexed with either $h\beta2m$ or $m\beta2m$ show that it is more stable than either an empty class I molecule or partially empty U_L18 (Fig. 3). The melting curves of the empty forms of class I and U_L18 were characterized by T_ms between 42 and 45°C, while the T_m of the m144-$h\beta2m$ curve was 55°C, closer to the T_m for peptide-filled K^d (56 to 57°C) (12, 13). m144 is slightly less stable when complexed with $m\beta2m$ ($T_m = 52$°C). This effect was also noted for the complex of $m\beta2m$ with K^d, compared with the complex of $h\beta2m$ with K^d (12), and more dramatically, for the complex of $m\beta2m$ with the nonclassical murine class I protein T10 (9). We were able to analyze the

effect of bound peptide on U_L18 stability by taking advantage of the fact that soluble U_L18 is only partially occupied with endogenous peptides when it is expressed at high levels. Addition of a synthetic peptide corresponding to the sequence of an endogenous peptide eluted from U_L18 shifts the T_m to 66°C, thus formally demonstrating that U_L18 binds this peptide and suggesting a general method for assaying peptide binding by U_L18.

The different properties of U_L18 and m144 revealed by this study do not, in and of themselves, undermine the contention that these molecules both function as surrogate class I proteins, capable of engaging NK cell inhibitory receptors and protecting cells that lack class I surface expression. Murine NK cell inhibitory receptors are homodimeric C-type lectin superfamily proteins, whereas the majority of characterized human inhibitory receptors are members of the immunoglobulin superfamily (reviewed in references 22 and 35). It is therefore conceivable that mouse NK inhibitory receptors would recognize features of mouse class I MHC molecules different from those recognized on human class I molecules by human inhibitory receptors. While there is no evidence yet of a direct interaction between a mouse inhibitory receptor and m144, recent results demonstrate that the presence of m144 interferes with NK cell-mediated clearance of virus-infected cells in vivo (14). The connection between U_L18 and human NK cells is less straightforward. A recent study reported that U_L18 expressed on a human class I-negative B-lymphoblastoid cell line inhibited NK cell lysis through interaction with the C-lectin-like inhibitory receptor CD94 (40). However, we and investigators at other laboratories have been unable to detect cell surface expression of U_L18 when its gene was transfected into the same B-cell line (31b). Additional results indicate that the presence of U_L18 on virus-infected fibroblasts slightly augments, rather than inhibits, NK cell-mediated lysis (31b). A probable host ligand for U_L18 was recently identified as LIR-1, a new immunoglobulin superfamily member related to human NK inhibitory receptors (8). LIR-1 is expressed mainly on B cells and monocytes, but only on a subset of NK cells; thus, it is possible that the HCMV MHC homolog exerts its primary effects on host cells other than NK cells. Further studies will be necessary to resolve the roles of both m144 and U_L18 in the interactions of their respective viruses with the immune systems of the infected hosts. However, currently available data suggest that the two homologs function differently, a hypothesis that is consistent with the biochemical and structural differences between m144 and U_L18 observed in the present study.

REFERENCES

1. **Bebbington, C. R., and C. C. G. Hentschel.** 1987. The use of vectors based on gene amplification for the expression of cloned genes in mammalian cells, p. 163–188. *In* D. M. Glover (ed.), DNA cloning: a practical approach. IRL Press, Oxford, United Kingdom.
2. **Beck, S., and B. G. Barrell.** 1988. Human cytomegalovirus encodes a glycoprotein homologous to MHC class I antigens. Nature **331:**269–272.
3. **Bjorkman, P. J., and P. Parham.** 1990. Structure, function and diversity of class I major histocompatibility complex molecules. Annu. Rev. Biochem. **90:**253–288.

4. **Bjorkman, P. J., M. A. Saper, B. Samraoui, W. S. Bennett, J. L. Strominger, and D. C. Wiley.** 1987. Structure of the human class I histocompatibility antigen, HLA-A2. Nature **329:**506–512.

5. **Britt, W. J., and C. A. Alford.** 1996. Cytomegalovirus, p. 2493–2523. *In* B. N. Fields, D. M. Knipe, P. M. Howley, R. M. Chanock, J. L. Melnick, T. P. Monath, B. Roizman, and S. E. Straus (ed.), Fields Virology. Lippincott-Raven, Philadelphia, Pa.

6. **Browne, H., G. Smith, S. Beck, and T. Minson.** 1990. A complex between the MHC class I homologue encoded by human cytomegalovirus and β2 microglobulin. Nature **347:**770–772.

7. **Burmeister, W. P., L. N. Gastinel, N. E. Simister, M. L. Blum, and P. J. Bjorkman.** 1994. Crystal structure at 2.2 Å resolution of the MHC-related neonatal Fc receptor. Nature **372:**336–343.

8. **Cosman, D., N. Fanger, L. Borges, M. Kubin, W. Chin, L. Peterson, and M.-L. Hsu.** 1997. A novel immunoglobulin superfamily receptor for cellular and viral MHC class I molecules. Immunity **7:**273–282.

9. **Crowley, M. P., Z. Reich, N. Mavaddat, J. D. Altmann, and Y.-H. Chien.** 1997. The recognition of the nonclassical major histocompatibility complex (MHC) class I molecule, T10, by the γδ T cell, G8. J. Exp. Med. **185:**1223–1230.

10. **Fahnestock, M. L., J. M. Dadgari, M. McMillan, and P. J. Bjorkman.** 1994. Phosphatidyl inositol-linked forms of a murine class I MHC molecule expressed on CHO cells retain peptide binding capability and alloreactivity. Int. Immunol. **6:**307–314.

11. **Fahnestock, M. L., J. L. Johnson, R. M. R. Feldman, J. M. Neveu, W. S. Lane, and P. J. Bjorkman.** 1995. The MHC class I homolog encoded by human cytomegalovirus binds endogenous peptides. Immunity **3:**583–590.

12. **Fahnestock, M. L., J. L. Johnson, R. M. R. Feldman, T. J. Tsomides, J. Mayer, L. O. Narhi, and P. J. Bjorkman.** 1994. Effects of peptide length and composition on binding to an empty class I MHC heterodimer. Biochemistry **33:**8149–8158.

13. **Fahnestock, M. L., I. Tamir, L. Narhi, and P. J. Bjorkman.** 1992. Thermal stability comparison of purified empty and peptide filled forms of a class I MHC molecule. Science **258:**1658–1662.

14. **Farrell, H. E., H. Vally, D. M. Lynch, P. Fleming, G. R. Shellam, A. A. Scalzo, and N. J. Davis-Poynter.** 1997. Inhibition of natural killer cells by a cytomegalovirus MHC class I homologue in vivo. Nature **386:**510–514.

15. **Gasser, D. L., K. A. Klein, E. Choi, and J. G. Seidman.** 1985. A new beta-2 microglobulin allele in mice defined by DNA sequencing. Immunogenetics **22:**413–416.

16. **Gastinel, L. N., N. E. Simister, and P. J. Bjorkman.** 1992. Expression and crystallization of a soluble and functional form of an Fc receptor related to class I histocompatibility molecules. Proc. Natl. Acad. Sci. USA **89:**638–642.

17. **Gates, F. T., J. E. Coligan, and T. J. Kindt.** 1981. Complete amino acid sequence of murine β2-microglobulin: structural evidence for strain-related polymorphism. Proc. Natl. Acad. Sci. USA **78:**554–558.

18. **Gorga, J. C., A. Dong, M. C. Manning, R. W. Woody, W. S. Caughey, and J. L. Strominger.** 1989. Comparison of the secondary structures of human class I and class II major histocompatibility complex antigens by Fourier-transform infrared and circular dichroism spectroscopy. Proc. Natl. Acad. Sci. USA **86:**2321–2325.

19. **Groh, V., S. Bahram, S. Bauer, A. Herman, M. Beauchamp, and T. Spies.** 1996. Cell stress-regulated human major histocompatibility complex class I gene expressed in gastrointestinal epithelium. Proc. Natl. Acad. Sci. USA **93:**12445–12450.

20. **Groves, M. L., and R. Greenberg.** 1982. Complete amino acid sequence of bovine β2-microglobulin. J. Biol. Chem. **257:**2619–2626.

21. **Harlow, E., and D. Lane.** 1988. Antibodies: a laboratory manual. Cold Spring Harbor Laboratory Press, Cold Spring Harbor, N.Y.

22. **Höglund, P., J. Sundback, M. Y. Olsson-Anheim, M. Johansson, M. Salcedo, C. Öhlén, H. G. Ljunggren, C. L. Sentman, and K. Kärre.** 1997. Host MHC class I control of NK-cell specificity in the mouse. Immunol. Rev. **155:**11–28.

23. **Holcombe, H. R., A. R. Castano, H. Cheroutre, M. Teitell, J. K. Maher, P. A. Peterson, and M. Kronenberg.** 1995. Nonclassical behavior of the thymus leukemia antigen—peptide transporter-independent expression of a nonclassical class I molecule. J. Exp. Med. **181:**1433–1443.

24. **Jardetzky, T. S., W. S. Lane, R. A. Robinson, D. R. Madden, and D. C. Wiley.** 1991. Identification of self peptides bound to purified HLA-B27. Nature **353:**325–330.

25. **Johnson, C. W.** 1990. Protein secondary structure and circular dichroism: a practical guide. Proteins Struct. Funct. Genet. **7:**205–214.

26. **Kabat, E. A., T. T. Wu, H. M. Perry, K. S. Gottesman, and C. Foeller.** 1991. Sequences of proteins of immunological interest. U.S. Department of Health and Human Services, Bethesda, Md.

27. **Kärre, K., H.-G. Ljunggren, G. Piontek, and R. Kiessling.** 1986. Selective rejection of H-2 deficient lymphoma variants suggest alternative immune defense strategy. Nature **319:**675–678.

28. **Kraulis, P. J.** 1991. MOLSCRIPT: a program to produce both detailed and schematic plots of protein structures. J. Appl. Crystallogr. **24:**946–950.

29. **Kunkel, T. A., J. D. Roberts, and R. A. Zakour.** 1987. Rapid and efficient site directed mutagenesis without phenotypic selection. Methods Enzymol. **154:**367–382.

30. **Lancet, D., P. Parham, and J. L. Strominger.** 1979. Heavy chain of HLA-A and HLA-B antigens is conformationally labile: a possible role for β2-microglobulin. Proc. Natl. Acad. Sci. USA **76:**3844–3848.

31. **Lanier, L. L., B. Corliss, and J. H. Phillips.** 1997. Arousal and inhibition of human NK cells. Immunol. Rev. **155:**145–154.

31a. **Lebrón, J. A., and P. J. Bjorkman.** Unpublished data.

31b. **Leong, C., T. L. Chapman, P. J. Bjorkman, E. Mocarski, and L. L. Lanier.** Unpublished data.

32. **Lin, A. Y., B. Devaux, A. Green, C. Sagerström, J. F. Elliott, and M. M. Davis.** 1990. Expression of T cell antigen receptor heterodimers in a lipid-linked form. Science **249:**677–679.

33. **Ljunggren, H. G., N. J. Stam, C. Öhlén, J. J. Neefjes, P. Höglund, M. T. Heemels, J. Bastin, T. N. M. Schumacher, A. Townsend, K. Kärre, and H. L. Ploegh.** 1990. Empty MHC class I molecules come out in the cold. Nature **346:**476–480.

34. **Merritt, E. A., and M. E. P. Murphy.** 1994. Raster3D version 2.0, a program for photorealistic molecular graphics. Acta Crystallogr. Sect. D **50:**869–873.

35. **Moretta, A., R. Biassoni, C. Bottino, D. Pende, M. Vitale, A. Poggi, M. C. Mingari, and L. Moretta.** 1997. Major histocompatibility complex class I-specific receptors on human natural killer and T lymphocytes. Immunol. Rev. **155:**105–117.

36. **Parham, P., M. J. Androlewicz, N. J. Holmes, and B. E. Rothenberg.** 1983. Arginine-45 is a major part of the determinant of human β2-microglobulin recognized by mouse monoclonal antibody BBM.1. J. Biol. Chem. **258:**6179–6186.

37. **Raghavan, M., L. N. Gastinel, and P. J. Bjorkman.** 1993. The class I MHC-related Fc receptor shows pH dependent stability differences correlating with immunoglobulin binding and release. Biochemistry **32:**8654–8660.

38. **Rammensee, H.-G., K. Falk, and O. Rötzschke.** 1993. Peptides naturally presented by MHC class I molecules. Annu. Rev. Immunol. **11:**213–244.

39. **Rawlinson, W. D., H. E. Farrell, and B. G. Barrell.** 1996. Analysis of the complete DNA sequence of murine cytomegalovirus. J. Virol. **70:**8833–8849.

40. **Reyburn, H. T., O. Mandelboim, M. Valez-Gomez, D. M. Davis, L. Pazmany, and J. L. Strominger.** 1997. The class I MHC homologue of human cytomegalovirus inhibits attack by natural killer cells. Nature **386:**514–519.

41. **Romero, P., G. Corradin, I. F. Luescher, and J. L. Maryanski.** 1991. H-2K^d restricted antigenic peptides share a simple binding motif. J. Exp. Med. **174:**603–612.

42. **Rötzschke, O., K. Falk, K. Deres, H. Schild, M. Norda, J. Metzger, G. Jung, and H.-G. Rammensee.** 1990. Isolation and analysis of naturally processed viral peptides as recognized by cytotoxic T cells. Nature **348:**252–257.

43. **Sambrook, J., E. F. Fritsch, and T. Maniatis.** 1989. Molecular cloning: a laboratory manual, 2nd ed. Cold Spring Harbor Laboratory Press, Cold Spring Harbor, N.Y.

44. **Sánchez, L. M., C. López-Otín, and P. J. Bjorkman.** 1997. Characterization and crystallization of human Zn-α2-glycoprotein, a soluble class I MHC homolog. Proc. Natl. Acad. Sci. USA **94:**4626–4630.

45. **Saper, M. A., P. J. Bjorkman, and D. C. Wiley.** 1991. Refined structure of the human histocompatibility antigen HLA-A2 at 2.6 Å resolution. J. Mol. Biol. **219:**277–319.

46. **Schumacher, T. N. M., M. T. Heemels, J. J. Neefjes, W. M. Kast, C. J. M. Melief, and H. L. Ploegh.** 1990. Direct binding of peptide to empty MHC class I molecules on intact cells and in vitro. Cell **62:**563–567.

47. **Stern, L. J., and D. C. Wiley.** 1994. Antigenic peptide binding by class I and class II histocompatibility proteins. Structure **15:**245–251.

48. **Tada, N., S. Kimura, A. Hatzfeld, and U. Hammerling.** 1980. Ly-m11: the H-3 region of mouse chromosome 2 controls a new surface alloantigen. Immunogenetics **11:**441–449.

49. **Townsend, A., and H. Bodmer.** 1989. Antigen recognition by class I-restricted T lymphocytes. Annu. Rev. Immunol. **7:**601–624.

50. **Townsend, A., T. Elliott, V. Cerundolo, L. Foster, B. Barber, and A. Tse.** 1990. Assembly of MHC class I molecules analyzed in vitro. Cell **62:**285–295.

51. **Van Bleek, G. M., and S. G. Nathenson.** 1990. Isolation of an endogenously processed immunodominant viral peptide from the class I H-2K^b molecule. Nature **348:**213–216.

52. **Weintraub, B. C., M. R. Jackson, and S. M. Hedrick.** 1994. Gamma-delta T-cells can recognize nonclassical MHC in the absence of conventional antigenic peptides. J. Immunol. **153:**3051–3058.